NRC Publications Archive
Archives des publications du CNRC

Kaolin polytypes revisited ab initio at 10 GPa
Mercier, Patrick H. J.; Le Page, Yvon; Desgreniers, Serge

NRC Publications Record / Notice d'Archives des publications de CNRC:
https://nrc-publications.canada.ca/eng/view/object/?id=7fbf414a-341a-404f-abe4-6b6b42444265
https://publications-cnrc.canada.ca/fra/voir/objet/?id=7fbf414a-341a-404f-abe4-6b6b42444265

National Research Council Canada   Conseil national de recherches Canada

Canada

Kaolin polytypes revisited ab initio at 10 GPa

P ATRICK H.J. M ERCIER, [1,*] Y VON L E P AGE, [1] AND S ERGE D ESGRENIERS [2]

[1]Institute for Chemical Process and Environmental Technology, National Research Council of Canada,
1200 Montreal Road, Ottawa, Ontario K1A 0R6, Canada
[2]Laboratoire de Physique des Solides Denses, Department of Physics, University of Ottawa,
150 Louis Pasteur, Ottawa, Ontario K1N 6N5, Canada

A BSTRACT

Based on systematic ab initio exploration, we reported last year that two new interlayer translations for kaolinite, $-\mathbf{a}/3$ and $(\mathbf{a}+\mathbf{b})/3$, allowed a new family of kaolin polytypes under moderate pressure. Both translations place each silicon atom of a kaolin layer on top of a hydroxyl group from the kaolin layer below, resulting in a triangular dipyramidal fivefold coordination to all silicon atoms. The predicted $-\mathbf{a}/3$ translation has since been independently observed experimentally at ~7 GPa, as kaolinite III phase, by compression of a natural kaolinite (Keokuk, Iowa). Encouraged by that verification, we extend here to the entire kaolin system both translations we had predicted for kaolinite. Based on calculated enthalpies and cell volumes for models optimized with ab initio density functional theory (DFT) calculations under pressure, we report three main results. First, we predict the existence of a kaolinite IV phase at a pressure not higher than 60 GPa and its likely crystal structure. Second, we predict three novel high-pressure crystal-structure models for nacrite, ranked by their enthalpy value, one of which is likely to be observed at about 10 GPa. Finally, three other novel and ranked high-pressure crystal-structure models are reported for dickite. Our results from interpretation of ab initio DFT calculations should guide experimental studies and facilitate their interpretation.

Keywords: Kaolin polytypes, kaolinite, dickite, nacrite, phase transitions, high pressure, ab initio DFT calculations

I NTRODUCTION

In a systematic ab initio DFT exploration, Mercier and Le Page (2008) (MLP8) rationalized low-energy phases in the kaolin system, based on an assumption of energy independence between non-neighboring layers. In the present letter, the MLP8 reference system for fractional atom coordinates is used throughout. Table 2 of MLP8 lists 72 possible low-energy phases at zero pressure, 36 of which are energy-distinguishable. The list includes all four kaolin polytypes then known: kaolinite, dickite, nacrite, and HP-dickite. A rough graph of enthalpy vs. pressure for all 36 phases (their Fig. 4) resulted from the list. All current reliable observations about synthesis, diagenesis, and phase transformations of members of the kaolin system were rationalized with this graph. In particular, the layer-slipping mechanism of Dera et al. (2003) for the reversible dickite ↔ HP-dickite transformation at ~2 GPa allowed rationalization of the observed existence of dickite at zero pressure and of the puzzling absence from the literature of reliable observations of any solid-to-solid transformation of kaolinite, dickite, or nacrite into each other under pressure.

In an extension of the work in MLP8, Mercier and Le Page (2009) (MLP9) assumed the generality of the layer-slipping mechanism for kaolin polytype transformations proposed by Dera et al. (2003). Application to a systematic search for post-kaolinite phases through an examination of 19 possible structure models has led MLP9 to the prediction of two prime candidate model phases

for post-kaolinite, one with space group symmetry $P1$ and the other with Cm at 12 GPa, both new structures (MLP9). They result, respectively, from new interlayer translations $-\mathbf{a}/3$ and $(\mathbf{a}+\mathbf{b})/3$, which were argued to only exist at high pressure (MLP9).

Upon application of pressure in a diamond anvil cell at room temperature, Welch and Crichton (2010) have recently observed two phase transitions in kaolinite from Keokuk (Iowa). The ambient phase (kaolinite I) transforms reversibly into kaolinite II at 3.7 GPa, whereas kaolinite II transforms irreversibly into kaolinite III at 7.8 GPa. Using powder diffraction data recalculated with the models from supplementary tables in MLP8 and MLP9, Welch and Crichton identified their kaolinite II phase as MLP8's model K5a [=MLP9 model (KT1)a] and their kaolinite III phase as the prime-candidate triclinic $P1$ phase for high-pressure kaolinite predicted by MLP9. This recent discovery of the kaolinite III phase has established experimentally the novel $-\mathbf{a}/3$ and by extension $(\mathbf{a}+\mathbf{b})/3$ translations, which were predicted by MLP9 to occur upon compression of kaolinite. We extend here in MLP8 fashion those interlayer translations from kaolinite to the whole system of kaolin polytypes at 10 GPa. In particular, we establish ab initio in this way the crystal structures that post-nacrite and post-HP-dickite phases are likely to adopt upon compression to about 10 GPa.

E XPERIMENTAL METHODS

Model building

Table 2 in MLP8 lists the combinations of the six possible $k\pi/3$ (k = 0–5) rotations $\mathbf{R}$ of the kaolin layers with the six interlayer translations $\mathbf{T}$ [0; $(2\mathbf{a}+\mathbf{b})/3$;

---

* E-mail: patrick.mercier@nrc-cnrc.gc.ca

($\mathbf{a}$+2$\mathbf{b}$)/3; $\mathbf{a}$/3; $\mathbf{b}$/3; and 2($\mathbf{a}$+$\mathbf{b}$)/3] that are possible at low pressure, and with two possible stacking sequences a and b. Stacking type a corresponds to the repeated application of the combined ($\mathbf{R}$,$\mathbf{T}$) operation while stacking type b corresponds to the repeated application of the succession of ($\mathbf{R}$,$\mathbf{T}$) and its enantiomorph ($\mathbf{R^*}$,$\mathbf{T^*}$). We carry out here the same exercise, but with the three translations that are possible at 10 GPa: –$\mathbf{a}$/3, its enantiomorphic operation –$\mathbf{b}$/3, and ($\mathbf{a}$+$\mathbf{b}$)/3, which is its own enantiomorphic operation. The translations are not in themselves enantiomeric, but generate enantiomeric structures when combined with $\mathbf{R^*}$. The resulting 36 corresponding models are given in Table 1. Only 18 of them are energy-distinguishable; those were optimized by DFT at 10 GPa. The polytype model construction follows closely the construction outlined in MLP8. The model in MLP8's Table 1c is the starting model to build kaolin polytypes at 10 GPa. We use here the labels [KP01]a to [KP23]b for the various models. All labels used start with a KP prefix (K for kaolin and P for pressure) to avoid confusion with models in MLP8 and MLP9 where prefixes K and KT were used, respectively. The first index in the label is the value of k in kπ/3 (k = 0–5) for the rotation $\mathbf{R}$. The second index is the sequence number for the translation in the order –$\mathbf{a}$/3, –$\mathbf{b}$/3, ($\mathbf{a}$+$\mathbf{b}$)/3. The last letter is a or b, meaning stacking type a or b above. In other words, models here can be recreated from the cell data and atom coordinates in MLP8's Table 1c and their label here.

Ab initio DFT calculations

All ab initio DFT calculations were performed with VASP (Kresse 1993; Kresse and Hafner 1993). All modeling, VASP input file preparation and output file interpretation was carried out with Materials Toolkit (Le Page and Rodgers 2005). The ab initio optimization procedure was identical to that in MLP8, with the exception of the introduction of a 10 GPa pressure in VASP by means of a corresponding Pulay stress (Pulay 1980).

RESULTS

Table 1 summarizes the various models and their final enthalpies at 10 GPa. Ideal and optimized cell data as well as atomic positions, obtained from ab initio DFT optimization for all models, are deposited as Supplementary Tables[1]. The same optimized models for just the kaolinite, nacrite, and dickite

families of polytypes are, respectively, printed in Tables 2a–2c[1], but rearranged—all silicate tetrahedra point along +z, the basal silicate oxygen atoms have zero z coordinate, and all representative atoms are selected in the same kaolin layer.

All pressures reported here are straight from VASP. From prior experience for calculations of many other materials, as explained in both MLP8 and MLP9, we know that pressures obtained by DFT calculations are likely to be biased toward higher values by about 2 or 3 GPa.

DISCUSSION

Translations upon compression

In kaolinite, MLP9 showed that the new interlayer translations –$\mathbf{a}$/3 and ($\mathbf{a}$+$\mathbf{b}$)/3 correspond to considerable enthalpy differences at high pressure with respect to the usual vectors as given for instance in MLP8. As the enthalpy difference clearly originates in the additional oxygen neighbor acquired by silicon atoms, it follows that this mechanism is not restricted to kaolinite, but could be more general in other kaolin polytypes under similar pressure. This mechanism repositions the center of the silicate ring over a hydroxyl from the top aluminate sheet of the kaolin layer below. There is only one silicate ring center (at 0,0,0.14) and three hydroxyls per kaolin (a,b) mesh at 2/3,0,0.65, 0,2/3,0.65, and 1/3,1/3,0.65 in the ideal kaolin model as presented in Table 1c in MLP8. As the silicate ring center is the origin of x and y, and thus remains fixed upon application of the rotation $\mathbf{R}$, it follows that only three translations $\mathbf{T}$, namely –$\mathbf{a}$/3, –$\mathbf{b}$/3, and ($\mathbf{a}$+$\mathbf{b}$)/3, can achieve the above atom repositioning.

Rotation upon compression

As the polytype transformations discussed here are solid-to-solid transformations, they cannot involve rotations of layers upon application of pressure as that would require macroscopic atom displacements. This is why kaolinite cannot transform into nacrite or into dickite or vice versa at any pressure without dissolution and recrystallization, even under conditions where those phases would have lower enthalpy. On the contrary, the translations discussed here involve shearing of layered materials by a few angstroms at most, and are thus plausible solid-to-solid phase transformations of which we already know three instances (dickite ↔ HP-dickite; kaolinite I ↔ kaolinite II; and kaolinite II → kaolinite III). Nacrite and dickite are, respectively, models K9b and K16b from MLP8. That places them, respectively, in columns 2 and 3 of MLP8's Table 2b. Transformation of nacrite then has to be to one of the three models in column 2 of Table 1b here and that of dickite must correspond to one of the three models in column 3 of Table 1b here. Transformation of kaolinite is different because a rotation by +0 is not different from a rotation by –0. It follows that kaolinite (model K11a in MLP8) at 10 GPa must then lead to one of the models in column 1 of either Table 1a or Table 1b here. As columns 2, 3, or 4 in Table

TABLE 1a. Repeated application of ($\mathbf{R}$,$\mathbf{T}$)

Translation $\mathbf{T}$	Rotation $\mathbf{R}$					
	0	π/3	2π/3	π	4π/3	5π/3
–$\mathbf{a}$/3	[KP01]a	[KP11]a	[KP21]a	[KP31]a	[KP22]a*	[KP12]a*
Space group	$P1$	$P6_1$	$P3_1$	$P2_1$		
H (eV/fu)	–105.645	–105.550	–105.609	–105.659		
V/fu (Å^3)	131.84	132.15	132.21	132.27		
–$\mathbf{b}$/3	[KP01]a*	[KP12]a	[KP22]a	[KP31]a*	[KP21]a*	[KP11]a*
Space group		$P6_1$	$P3_1$			
H (eV/fu)		–105.642	–105.539			
V/fu (Å^3)		132.59	132.21			
($\mathbf{a}$+$\mathbf{b}$)/3	[KP03]a	[KP13]a	[KP23]a	[KP33]a	[KP23]a*	[KP13]a*
Space group	Cm	$P6_1$	$P3_1$	$Cmc2_1$		
H (eV/fu)	–105.576	–105.632	–105.620	–105.579		
V/fu (Å^3)	131.51	132.25	132.14	131.61		

TABLE 1b. Repeated application of the sequence [($\mathbf{R}$,$\mathbf{T}$):($\mathbf{R^*}$,$\mathbf{T^*}$)]

Translation $\mathbf{T}$	Rotation $\mathbf{R}$					
	0	π/3	2π/3	π	4π/3	5π/3
–$\mathbf{a}$/3	[KP01]b	[KP11]b	[KP21]b	[KP31]b	=[KP22]b	=[KP12]b
Space group	Cc	Cc	Cc	Cc		
H (eV/fu)	–105.608	–105.557	–105.622	–105.636		
V/fu (Å^3)	131.88	132.10	131.62	132.38		
–$\mathbf{b}$/3	=[KP01]b	[KP12]b	[KP22]b	=[KP31]b	=[KP21]b	=[KP11]b
Space group		Cc	Cc			
H (eV/fu)		–105.633	–105.535			
V/fu (Å^3)		131.93	131.84			
($\mathbf{a}$+$\mathbf{b}$)/3	=[KP03]a	[KP13]b	[KP23]b	=[KP33]a	=[KP23]b	=[KP13]b
Space group	Cm	Cc	Cc	$Cmc2_1$		
H (eV/fu)	–105.576	–105.648	–105.624	–105.579		
V/fu (Å^3)	131.51	132.24	131.76	131.62		

1a, or column 4 in Table 1b do not correspond to kaolin polytypes observed at room pressure or at any pressure, they are listed here for completeness, as possible new kaolin polytypes. Corresponding models, cell volumes, and enthalpies are found in the Supplementary Tables[1].

Energy independence between layers

The polytype derivation done here follows that of MLP8, where the energy independence between non-neighboring layers is assumed. The fact that all six kaolin polytypes known today (including kaolinites II and III) are consistent with this assumption can hardly be a coincidence. The list of possible polytypes in Table 1 here is accordingly short. If the energy independence between up to second-neighbor layers only had been assumed as it was the case in MLP9, this list would be much longer. We accordingly felt justified to limit the search here to models that would also be consistent with the assumption of the energy independence between non-neighboring layers; results of future experiments could corroborate or reject this assumption. If experiments at 10 GPa with nacrite and dickite produced phases not reported in Tables 2b and 2c[1], respectively, extension of the reasoning here in MLP9 fashion could then be applied to explore many more possible low-enthalpy stackings and hopefully conclusively identify the observed experimental polytype.

Enthalpies at 10 Ga

The spread of calculated enthalpies $H = U + PV$, where U is the free energy of a volume V of matter under pressure P, is a mere 124 meV/formula unit (fu), i.e., less than 12 kJ/mol for all models in Table 1. As in MLP8, we evaluated the standard uncertainty of our calculations to be 13 meV (~1.25 kJ/mol). This small spread allows ranking of the plausible phases, but without ruling out any of the phases. Calculated enthalpies in Table 1 predict kaolinite to adopt the structure of model [KP01]a with symmetry $P1$ at 10 GPa, as shown in Table 2a[1], in strong preference to model [KP03]a with symmetry Cm, as its enthalpy is calculated to be higher by 69 meV/fu, while that of the [KP01]b Cc model is higher by only 40 meV. Model [KP01]a corresponds to the triclinic $P1$ structure predicted by MLP9 and observed for kaolinite III by Welch and Crichton (2010), as it should. Enthalpies in Table 1 also predict nacrite to adopt the structure of model [KP13]b (Table 2b[1]) with a slight preference to model [KP12]b and to [KP11]b in that order, respectively, with enthalpies that are higher by 15 and 91 meV/fu. Similarly dickite should correspond to either model [KP21]b or [KP23]b with nearly identical enthalpies (Table 2c[1]) in strong preference to [KP22]b with an enthalpy that is 89 meV/fu higher.

Cell volumes and evolution of enthalpy with pressure

Phase stability relates to the phase with lowest enthalpy under a given set of pressure and temperature conditions. Polytype evolution of layered materials upon compression is about phases with same layer rotations (i.e., same column in either Tables 1a or 1b) and lower enthalpy. Values for free energy and cell volumes at zero pressure allowed MLP8 to derive a graph of phase stability and phase evolution at moderate pressures (their Fig. 4). Based on their graph in Figure 4b, Mercier and Le Page (2008) discuss the evolution of dickite into HP dickite, but the prediction of a solid-to-solid transformation of kaolinite into phase [K5a] (=phase [KT1]a in MLP9) at about 5.5 GPa can also be read off the same graph.

Upon compression of kaolinite in a diamond-anvil cell, Welch and Crichton (2010) observed the formation of kaolinite II at 2.7 GPa and kaolinite III at 7.8 GPa. They identified them as, respectively, models [K5a] from MLP8 and "P1" from MLP9. Similarly, as model [KP01]a with volume per formula unit of 131.84 Å^3 is observed to form first as kaolinite III at 7.8 GPa, the smaller volume of 131.51 Å^3 for model [KP03]a suggests the existence of an even denser phase, kaolinite IV, at higher pressure. Cell volume and enthalpy calculations for higher pressures show this conclusion to be ultimately correct, however the complete story (Table 3[1] and Fig. 1) is much more complicated than a linear extrapolation calculated from energy and cell volume as in MLP8. The Cm phase becomes more stable than the $P1$ phase (Fig. 1a), but not before a pressure of ~57 GPa because the Cm phase itself experiences cell-volume (Fig. 1b) and cell-parameter (Fig. 1c) discontinuities between 22.5 and 25
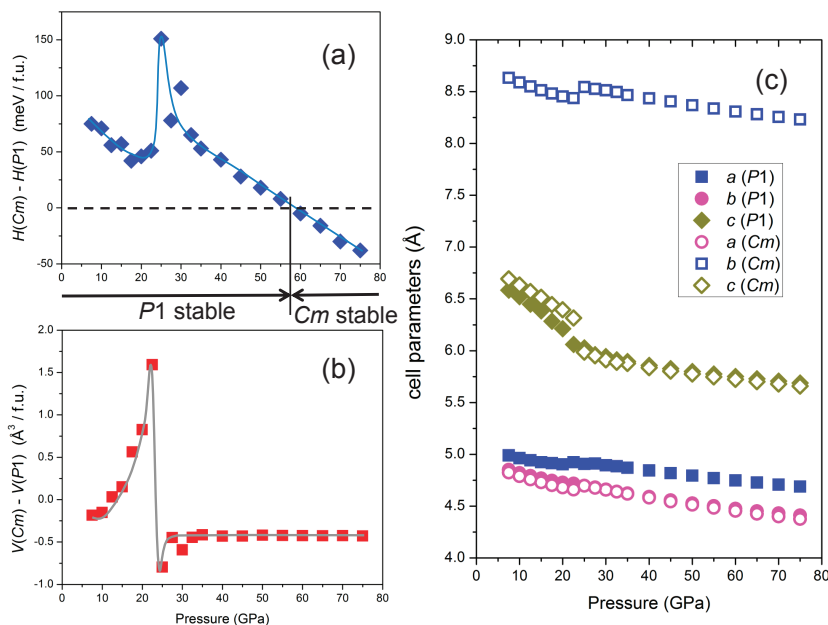

FIGURE 1. (**a**) Evolution with pressure of the enthalpy difference between models [KP03]a (kaolinite IV) and [KP01]a (kaolinite III). Stable refers to polytype stability upon interlayer translations, not to overall stability in the whole kaolin system. (**b**) Same for cell volumes. (**c**) Same for cell parameters a, b, and c. The cell-volume and cell-parameter discontinuities of the Cm phase between 22.5 and 25 GPa correspond to the point where the Si atoms come close to the plane of basal oxygen atoms (see Fig. 2).
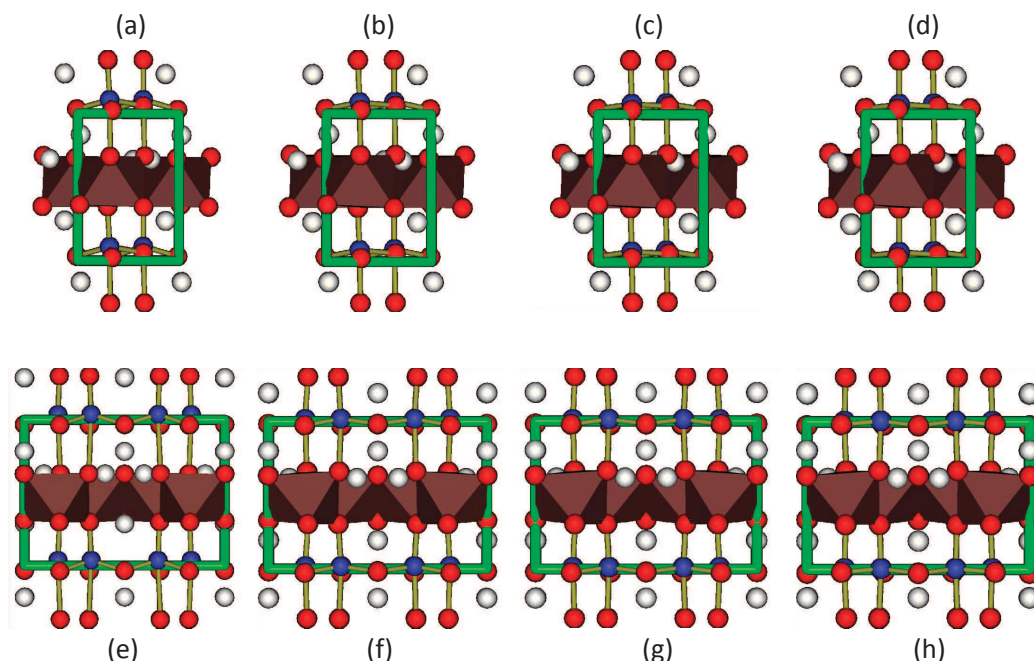
FIGURE 2. [100] views with c up for *P*1 structures: (**a**) 20 GPa, (**b**) 25 GPa, (**c**) 35 GPa, (**d**) 60 GPa. [100] views with c down for *Cm* structures: (**e**) 20 GPa, (**f**) 25 GPa, (**g**) 35 GPa, (**h**) 60 GPa. The green boxes outline the unit cell.

GPa. These discontinuities correspond to the point where the Si atoms come close to the plane of basal oxygen atoms (Fig. 2). A transformation to the *Cm* phase is not an established fact, but we can safely predict that kaolinite III will be unstable at pressures greater than 60 GPa, as we know a model with lower enthalpy at that pressure. The enthalpy difference between the [KP01]b and [KP01]a models increases monotonically with pressure up to 75 GPa, forbidding the existence of a [KP01]b phase at any pressure up to that pressure.

The experimental observation of diffraction patterns for the dense phases of nacrite and dickite at pressures of about 10 GPa will provide tests for our calculations and incentives to model other phases at higher pressures.

Usefulness of rational structure modeling in parallel with ab initio DFT calculations

We have explored the possible phases of minerals of the kaolin system at 10 GPa under an assumption of the energy independence between non-neighboring layers, leading to ab initio compression of only 18 models for the entire kaolin system. We have confirmed that the expected crystal structure for kaolinite at 10 GPa is the *P*1 structure that we predicted earlier in MLP9, and that was observed for kaolinite III by Welch and Crichton (2010) at 7.8 GPa. We accordingly predict a transition to a kaolinite IV phase at pressures no higher than 60 GPa. It could have the crystal structure of model [KP03]a with space group *Cm*. We also propose and rank here three possible structure models each for nacrite and dickite at pressures of about 10 GPa. Our model predictions await an experimental confirmation.

The DFT structure-prediction exercises in Mercier and Le Page (2008, 2009) seem to have been useful as MLP8 may have promoted experimental work like that of Welch and Crichton

(2010) while both MLP8 and MLP9 probably facilitated the structure identifications in it. We hope that the present contribution will similarly demonstrate the usefulness of rational modeling complemented by ab initio DFT calculations for guidance and interpretation of experiments in experimentally difficult systems such as the kaolin system.

REFERENCES CITED

Dera, P., Prewitt, C.T., Japel, S., Bish, D.L., and Johnston, C.T. (2003) Pressure-controlled polytypism in hydrous layered materials. American Mineralogist, 88, 1429–1425.
Kresse, G. (1993) Ab initio molekular dynamik für flüssige metalle. Ph.D. thesis. Technische Universität Wien, Austria.
Kresse, G. and Hafner, J. (1993) *Ab initio* molecular dynamics for open-shell transition metals. Physical Review B, 48, 13115–13118.
Le Page, Y. and Rodgers, J.R. (2005) Quantum software interfaced with crystal-structure databases: tools, results and perspectives. Journal of Applied Crystallography, 38, 697–705.
Mercier, P.H.J. and Le Page, Y. (2008) Kaolin polytypes revisited *ab initio*. Acta Crystallographica B, 64, 131–143.
——— (2009) *Ab initio* exploration of layer slipping transformations in kaolinite up to 60 GPa. Materials Science and Technology, 25, 437–442.
Pulay, P. (1980) Convergence acceleration of iterative sequences. The case of scf iteration. Chemical Physics Letter, 73, 393–398.
Welch, M.D. and Crichton, W.A. (2010) Pressure-induced transformations in kaolinite. American Mineralogist, 95, 651–654.